JCB Article

Role of the mammalian retromer in sorting of the cation-independent mannose 6-phosphate receptor

Cecilia N. Arighi,[1] Lisa M. Hartnell,[1] Ruben C. Aguilar,[1] Carol R. Haft,[2] and Juan S. Bonifacino[1]

[1]Cell Biology and Metabolism Branch, National Institute of Child Health and Human Development, and [2]Division of Diabetes, Endocrinology, and Metabolism, National Institute of Diabetes and Digestive and Kidney Diseases, National Institutes of Health, Bethesda, MD 20892

The cation-independent mannose 6-phosphate receptor (CI-MPR) mediates sorting of lysosomal hydrolase precursors from the TGN to endosomes. After releasing the hydrolase precursors into the endosomal lumen, the unoccupied receptor returns to the TGN for further rounds of sorting. Here, we show that the mammalian retromer complex participates in this retrieval pathway. The hVps35 subunit of retromer interacts with the cytosolic domain of the CI-MPR. This interaction probably occurs in an endosomal compartment, where most of the retromer is localized. In particular, retromer is associated with tubular–vesicular profiles that emanate from early endosomes or from intermediates in the maturation from early to late endosomes. Depletion of retromer by RNA interference increases the lysosomal turnover of the CI-MPR, decreases cellular levels of lysosomal hydrolases, and causes swelling of lysosomes. These observations indicate that retromer prevents the delivery of the CI-MPR to lysosomes, probably by sequestration into endosome-derived tubules from where the receptor returns to the TGN.

Introduction

Like other basic cellular processes, the mechanisms by which newly synthesized acidic hydrolases are sorted to the yeast vacuole and the mammalian lysosome are evolutionarily conserved. In the yeast *Saccharomyces cerevisiae*, this sorting is initiated by the binding of soluble hydrolase precursors such as pro-carboxypeptidase Y and pro-proteinase A to the transmembrane receptor Vps10p in the late Golgi complex (Marcusson et al., 1994; Cooper and Stevens, 1996). The hydrolase–Vps10p complexes are then transported to a late endosomal or prevacuolar compartment by a process that is at least partially dependent on the coat proteins, clathrin (Seeger and Payne, 1992; Deloche et al., 2001), Golgi-localized, γ ear–containing ARF-binding proteins (Dell'Angelica et al., 2000; Hirst et al., 2000, 2001; Costaguta et al., 2001; Mullins and Bonifacino, 2001; Zhdankina et al., 2001), and AP-1 (Costaguta et al., 2001; Hirst et al., 2001). The acidic environment of the prevacuolar compartment induces dissociation of the hydrolase–Vps10p complexes, after which the hydrolases are transported to the vacuole and the pro sequences are removed by proteolytic cleavage, while Vps10p returns to the late Golgi complex to mediate further rounds of sorting (Cooper and Stevens, 1996; Seaman et al., 1997). Emr and colleagues demonstrated that Vps10p retrieval is mediated by a heteropentameric complex named "retromer" (Seaman et al., 1998). The yeast retromer comprises five cytosolic/peripheral membrane proteins termed Vps5p, Vps17p, Vps26p, Vps29p, and Vps35p (Seaman et al., 1998). Vps35p recognizes the cytosolic domain of Vps10p and forms a stable subcomplex with Vps29p (Nothwehr et al., 1999, 2000). Vps5p and Vps17p contain Phox homology domains that bind phosphatidylinositol 3-phosphate, and interact with one another to form another stable subcomplex. This Vps5p–Vps17p subcomplex has a tendency to oligomerize and has therefore been proposed to serve as a scaffold for the assembly of a putative membrane coat that drives vesicle formation (Horazdovsky et al., 1997; Seaman et al., 1998; Seaman and Williams, 2002). Finally, Vps26p has been proposed to promote the assembly of the cargo-selective

The online version of this article includes supplemental material.

Address correspondence to Juan S. Bonifacino, Cell Biology and Metabolism Branch, National Institute of Child Health and Human Development, Building 18T/Room 101, National Institutes of Health, Bethesda, MD 20892. Tel.: (301) 496-6368. Fax: (301) 402-0078. email: juan@helix.nih.gov

R.C. Aguilar's present address is Department of Biology, The Johns Hopkins University, 3400 North Charles Street, Baltimore, MD 21218.

Key words: lysosomal enzymes; multivesicular bodies; sorting nexins; yeast vacuole; clathrin adaptors

Abbreviations used in this paper: CD-MPR, cation-dependent mannose 6-phosphate receptor; CI-MPR, cation-independent mannose 6-phosphate receptor; MPR, mannose 6-phosphate receptor; PACS-1, phosphofurin acidic cluster sorting protein-1; siRNA, small interfering RNA; Snx, sorting nexin; TfR, transferrin receptor; TIP47, tail-interacting protein of 47 kD.

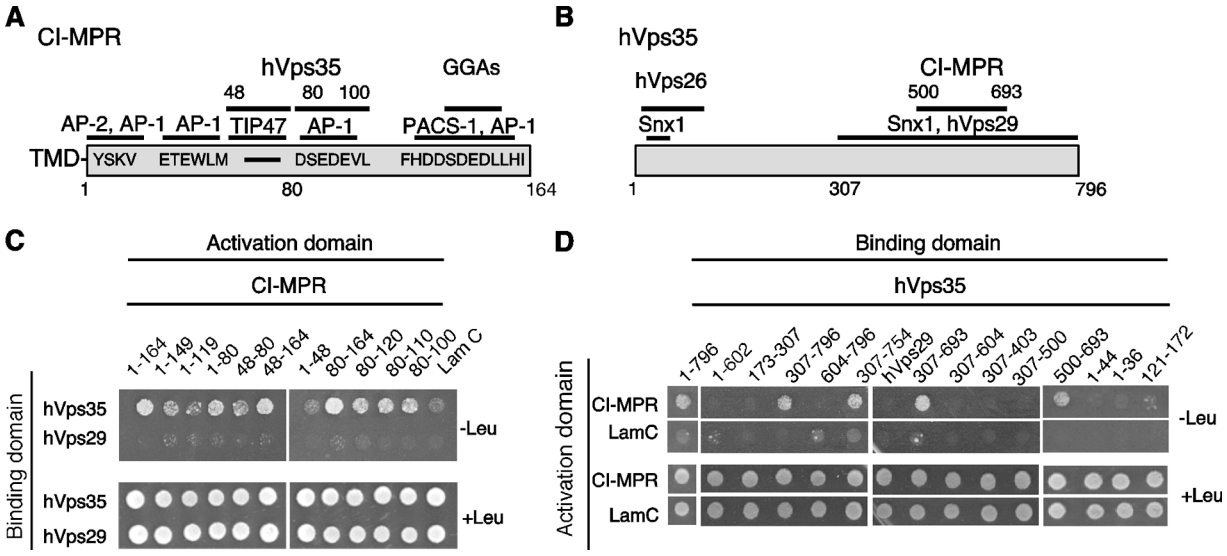

Figure 1. **hVps35 binds to the cytosolic domain of the CI-MPR.** (A) Schematic representation of the cytosolic domain of the CI-MPR indicating binding sites for interaction partners involved in sorting. (B) Schematic representation of hVps35 indicating segments that bind to other retromer subunits and to the CI-MPR. (C and D) Yeast two-hybrid analyses showing the interaction of full-length hVps35 with segments of the CI-MPR cytosolic domain, and the interaction of the full-length CI-MPR cytosolic domain with fragments of hVps35. Interaction of the fusion proteins was detected by growth of cotransformed cells in the absence of leucine (−Leu) as described in the Materials and methods. hVps29 and lamin C were used as negative controls.

Vps35p–Vps29p subcomplex with the structural Vps5p–Vps17p subcomplex (Reddy and Seaman, 2001).

The functional counterparts of Vps10p in mammals are two transmembrane mannose 6-phosphate receptors (MPRs), namely the cation-dependent MPR (CD-MPR) and cation-independent MPR (CI-MPR; Kornfeld and Mellman, 1989; Ghosh et al., 2003). The names of these receptors derive from their ability to bind mannose 6-phosphate groups on the lysosomal hydrolase precursors in a divalent cation-dependent or -independent manner, respectively. This binding takes place at the TGN, which is the mammalian equivalent to the yeast late Golgi. The cytosolic domains of the MPRs have COOH-terminal acidic cluster–dileucine signals that bind Golgi-localized, γ ear–containing ARF-binding proteins (Puertollano et al., 2001; Takatsu et al., 2001; Zhu et al., 2001) and other less well-characterized signals that bind AP-1 (Glickman et al., 1989; Mauxion et al., 1996; Honing et al., 1997). These interactions are thought to cooperate in the packaging of hydrolase–MPR complexes into clathrin-coated vesicles or pleiomorphic carriers that bud from the TGN and deliver the complexes to either early or late endosomes (Geuze et al., 1985; Bock et al., 1997; Klumperman et al., 1998; Doray et al., 2002; Puertollano et al., 2003; Waguri et al., 2003). As described in the previous paragraph for yeast, the hydrolase–MPR complexes dissociate at the acidic pH of endosomes, upon which the hydrolases are carried with the fluid phase to the lysosome lumen while the MPRs recycle to the TGN. Several proteins and protein complexes have been implicated in endosome-to-TGN retrieval of MPRs in mammalian cells. Among these are the AP-1 complex (Meyer et al., 2000, 2001)—which thus seems to be involved in both forward and retrograde transport—and two adaptor-like proteins: tail-interacting protein of 47 kD (TIP47; Diaz and Pfeffer, 1998; Krise et al., 2000; Orsel et al., 2000) and phosphofurin acidic cluster sorting protein-1 (PACS-1; Wan et al., 1998). Intriguingly, mutations in yeast AP-1 alone do not impair pro-carboxypeptidase Y trafficking to the vacuole, implying normal recycling of Vps10p (Yeung et al., 1999). Furthermore, TIP47 and PACS-1 have no homologues in yeast. These findings could point to either important mechanistic differences between endosome-to-TGN transport in yeast and mammals or to the existence of evolutionarily conserved components of the MPR retrieval machinery that remain to be identified.

These considerations led us to hypothesize that the mammalian retromer could be involved in MPR trafficking. Indeed, structural homologues of all the yeast retromer subunits (except for Vps17p) have been identified in mammals (Haft et al., 2000). Despite the absence of a Vps17p homologue, the mammalian retromer is also thought to comprise five subunits, namely hVps26p, hVps29p, and hVps35p ("h" prefix designates "human"), plus two Vps5p homologues, the sorting nexins 1 and 2 (Snx1 and Snx2, respectively). The subunit interactions, tendency to oligomerization, and overall structure are similar to those of the yeast retromer components (Horazdovsky et al., 1997; Haft et al., 1998, 2000; Kurten et al., 2001; Seaman and Williams, 2002). Here, we demonstrate that the mammalian retromer has an important role in the trafficking of the CI-MPR.

Results

Interaction of the cytosolic domain of the CI-MPR with hVps35

Genetic and biochemical analyses have identified Vps35p as the cargo recognition component of the yeast retromer (Nothwehr et al., 2000). To determine whether this function is conserved in mammals, we tested for interaction of the 164-residue cytosolic domain of the CI-MPR (Fig. 1 A) with

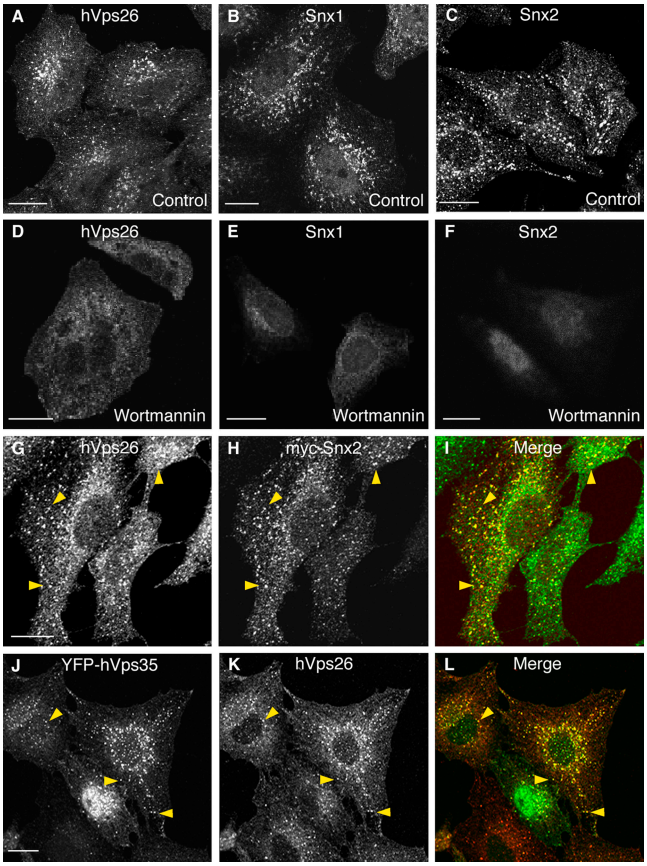

Figure 2. **Immunofluorescence microscopy analysis of the localization of retromer subunits.** (A–F) HeLa cells were incubated for 30 min at 37°C in the absence (A–C) or presence (D–F) of 100 nM wortmannin. Cells were then fixed and stained with rabbit pAbs to endogenous hVps26 (A and D), Snx1 (B and E), or Snx2 (C and F), followed by donkey Alexa® 488–conjugated anti–rabbit Igs. (G–I) HeLa cells transiently transfected with myc-Snx2 were costained for endogenous hVps26 as described above (G), and for myc-Snx2 using a mouse mAb to the myc epitope and donkey Cy3-conjugated anti–mouse Igs (H). (J–L) M1 cells stably transfected with YFP-hVps35 were stained for hVps26 as described above. Arrowheads indicate structures where hVps26 colocalizes with myc-Snx2 (G–I) and with YFP-hVps35 (J–L). Bars, 10 μm.

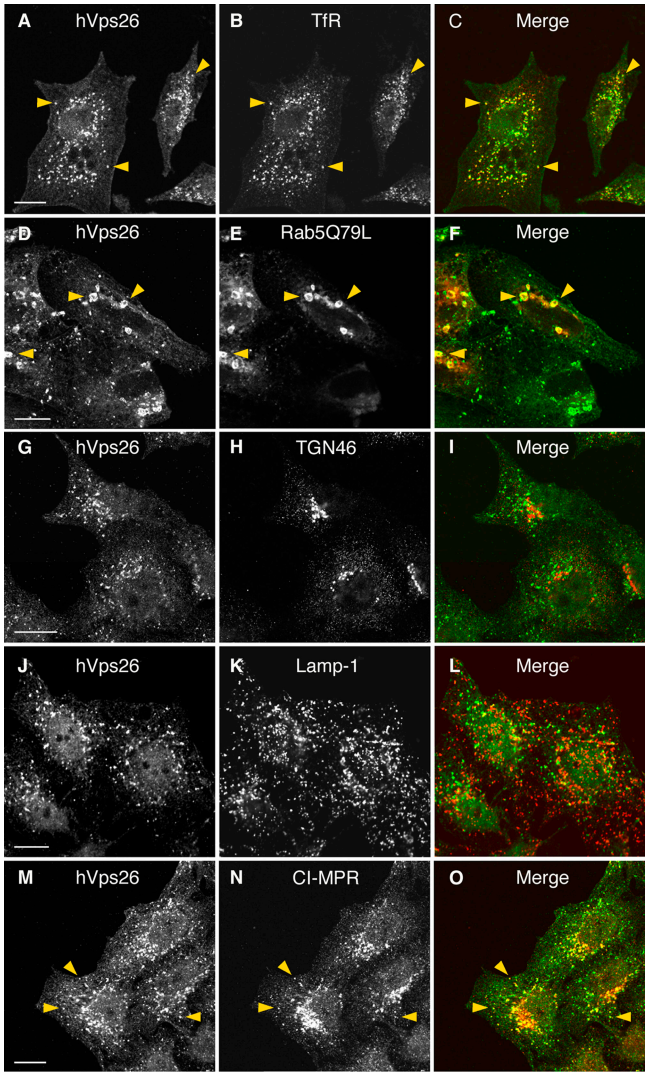

Figure 3. **Colocalization of hVps26 with organellar markers.** HeLa cells were fixed and costained with a rabbit pAb to hVps26 (A, D, G, J, and M), and with mouse mAbs to the TfR (B), TGN46 (H), Lamp-1 (K), and the CI-MPR (N), followed by donkey Alexa® 488–conjugated anti–rabbit and donkey Cy3-conjugated anti–mouse Igs. CFP-Rab5Q79L was expressed by transient transfection (E). Arrowheads indicate structures where two proteins colocalize. Bars, 10 μm.

hVps35 (Fig. 1 B). This analysis was conducted using the LexA-based yeast two-hybrid system, which is especially suited for the detection of low affinity interactions. Colony growth assays showed that hVps35 and the CI-MPR cytosolic domain do interact (Fig. 1 C). No interactions were observed when these constructs were replaced by hVps29 or lamin C, respectively, indicating that the hVps35–CI-MPR interaction is specific (Fig. 1 C). We also did not detect interaction between the CI-MPR cytosolic domain and hVps26 (unpublished data). The determinants of interactions were mapped by testing deletion mutants of the CI-MPR cytosolic domain and hVps35. Two nonoverlapping regions comprising cytosolic domain residues 48–80 and 80–100 of the CI-MPR cytosolic domain were found to be independently sufficient for interactions with hVps35 (Fig. 1 C), indicating the existence of two binding sites for hVps35 on the CI-MPR domain. Many amino acid substitutions within each of these regions abrogated binding (unpublished data), indicating that the binding determinants are complex and possibly conformational. Notably, the 48–100 region does not contain the YSKV sequence (residues 26–29) involved in internalization of the CI-MPR or the acidic cluster–dileucine motif (residues 153–162) implicated in its sorting at the TGN (Fig. 1, A and C; Ghosh et al., 2003). The region of hVps35 that binds to the cytosolic domain of CI-MPR was similarly mapped to the segment comprising residues 500–693 (Fig. 1 D). Thus, these experiments demonstrated an interaction between residues 48–100 of the CI-MPR cytosolic domain and residues 500–693 of hVps35.

Partial colocalization of retromer and CI-MPR on endosomes

The interactions described above prompted us to examine the potential involvement of retromer in CI-MPR traffick-

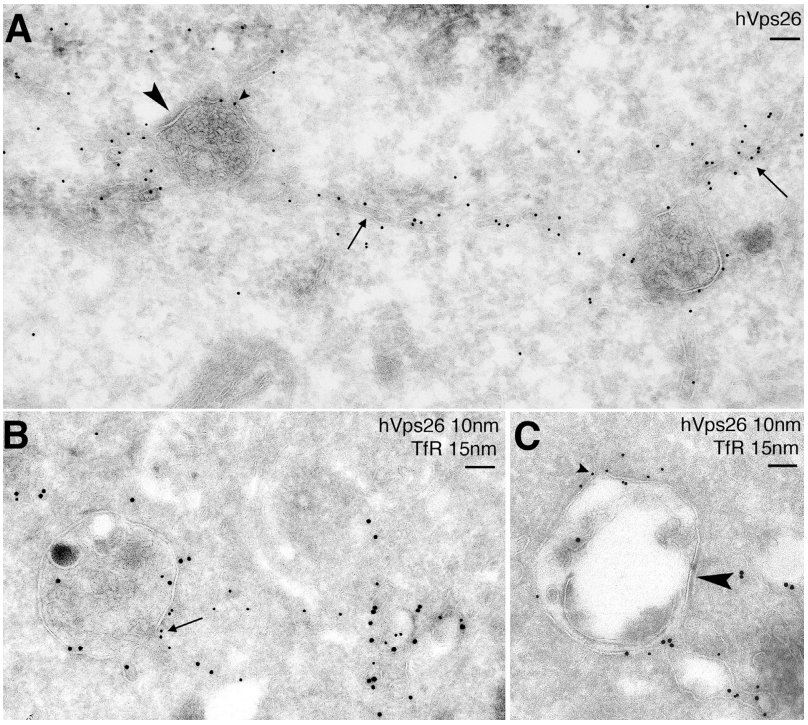

Figure 4. **Immuno-EM localization of hVps26 and TfR.** Ultrathin cryosections of HeLa cells were immunogold labeled with anti-hVps26 (A) or double-immunogold labeled with anti-hVps26 (10-nm gold particles) and anti-TfR (B and C, 15-nm gold particles). Arrows indicate the localization of hVps26 to tubular structures; large arrowheads indicate the presence of a bilayered clathrin coat on multivesicular endosomes; small arrowheads show the presence of hVps26 at the neck of tubules originating from endosomes. TfR colocalizes with hVps26 both in the tubules and in the endosomes. Bars, 100 nm.

ing. We started by determining the subcellular localization of endogenous retromer relative to various organellar markers, including the CI-MPR. Immunofluorescence microscopy with antibodies to three retromer subunits, hVps26, Snx1, and Snx2, showed a similar punctate staining of the cytoplasm in HeLa cells (Fig. 2, A–C). A 30-min treatment with the phosphatidylinositol 3-kinase inhibitor wortmannin resulted in loss of the punctate staining for all three proteins (Fig. 2, D–F). This result was consistent with the expected requirement of phosphatidylinositol 3-phosphate for association of the Snx proteins to membranes (Zhong et al., 2002). Double-labeling experiments showed that endogenous hVps26 colocalized with transgenic myc-tagged Snx2 (Fig. 2, G–I) and with transgenic hVps35 tagged with YFP (Fig. 2, J–L), indicating that the punctate staining observed for all of these proteins reflects the distribution of the retromer complex.

Additional experiments revealed extensive colocalization of endogenous hVps26 with the transferrin receptor (TfR), an early endosomal marker (Fig. 3, A–C; arrowheads). hVps26 was also found to localize to early endosomes enlarged by expression of the constitutively active Rab5Q79L mutant (Stenmark et al., 1994; Fig. 3, D–F). In contrast, we observed little or no colocalization of hVps26 with the TGN marker TGN46 (Fig. 3, G–I) or the late endosomal/lysosomal marker Lamp-1 (Fig. 3, J–L). The CI-MPR has been previously shown to distribute to the TGN and endosomes at steady state (Geuze et al., 1988; Klumperman et al., 1993). hVps26 exhibited partial colocalization with the CI-MPR, particularly in peripheral cytoplasmic foci (Fig. 3, M–O; arrowheads). From these experiments, we concluded that hVps26 (and, by extension, the retromer complex) is mainly localized to endosomes, where it partially colocalizes with a peripheral population of CI-MPR.

Association of retromer with tubular profiles adjacent to endosomes

The localization of retromer was analyzed at higher resolution by cryo-gold immuno-EM using a pAb to hVps26. Most of the hVps26 labeling (275 out of 365 gold particles counted, or 75%) was observed in association with tubular profiles in the vicinity of organelles that had the appearance of endosomes. Some of these organelles had a relatively clear lumen, whereas others contained intraluminal vesicles (Fig. 4, A and B). The tubules were often connected to the vacuolar portion of the organelles (Fig. 4, A and B; arrows). A smaller fraction of hVps26 (90 out of 365 gold particles counted, or 25%) was found on the limiting membrane of the endosomes themselves (Fig. 4, A–C), in some cases concentrated at the necks of protruding tubules (Fig. 4 A, small arrowhead). The multivesicular organelles often exhibited thick, flat coats resembling the "bilayered" clathrin- and Hrs-containing coats previously implicated in sorting to the ubiquitin–multivesicular body pathway (Raposo et al., 2001; Raiborg et al., 2002; Sachse et al., 2002; Fig. 4, A and C, large arrowhead). Retromer was not excluded from these bilayered coats, although it tended to concentrate on other domains of the organelle membrane adjacent to emerging tubules.

To characterize these structures in more detail, we performed double labeling for hVps26 and other organellar markers. The multivesicular endosomes that contained hVps26 also labeled for the TfR, indicating that they corresponded to an early endosomal compartment (Fig. 4, B and C). The CI-MPR was found in the intraluminal vesicles of the endosomes as well as in the retromer-containing tubules emanating from these endosomes (Fig. 5 A), a distribution that was in agreement with that observed in previous papers (Geuze et al., 1988; Klumperman et al., 1993). We did not

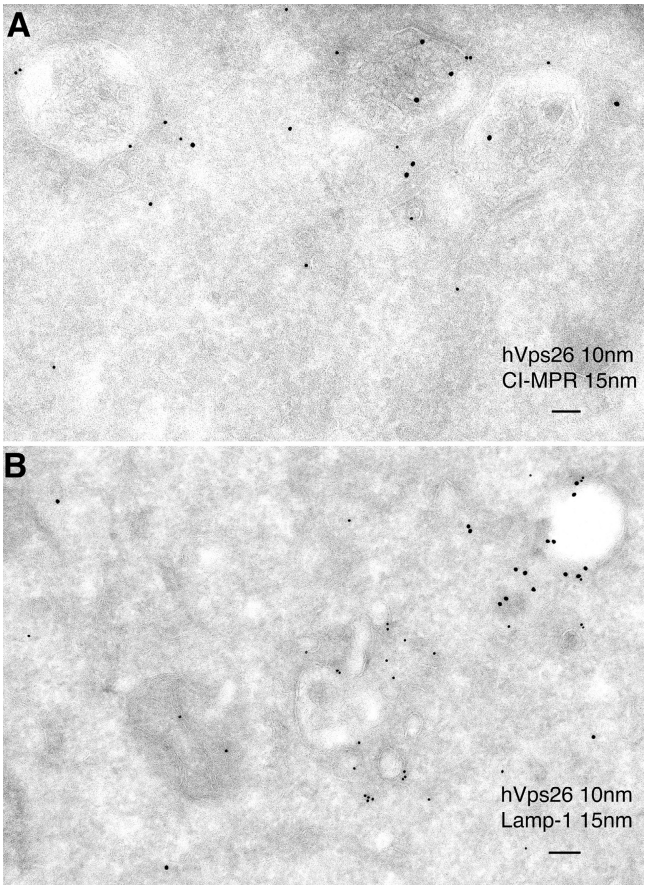

Figure 5. **Immuno-EM localization of hVps26 relative to CI-MPR and Lamp-1.** Ultrathin cryosections of HeLa cells were double-immunogold labeled with anti-hVpS26 (10-nm gold particles) and either anti-CI-MPR or Lamp-1 (15-nm gold particles) (A and B, respectively). Notice the partial colocalization of hVps26 with CI-MPR in multivesicular endosomes (A). The endosomes that are labeled with hVps26 are devoid of Lamp-1 (B), pointing to the early endosomal nature of these structures. Bars, 100 nm.

observe significant colocalization of retromer with Lamp-1 (Fig. 5 B), ruling out an association of retromer with mature late endosomes and lysosomes. From these observations, we concluded that retromer is mainly associated with the previously described bilayered coated endosomes, which represent an intermediate stage in the maturation of early to late endosomes (Raposo et al., 2001; Raiborg et al., 2002; Sachse et al., 2002). The tubules emanating from these endosomes are likely the conduits through which the CI-MPR transits on its way back to the TGN, as previously proposed (Geuze et al., 1988).

In vivo dynamics of retromer-containing structures

The dynamics of retromer-containing structures were examined by live imaging of M1 cells expressing YFP-hVps35 (Fig. 6). Immunoprecipitation-recapture experiments demonstrated that YFP-hVps35 was efficiently incorporated into the retromer complex (unpublished data), and thus reflected the behavior of the complex. Indeed, the cytoplasmic punctate distribution of YFP-hVps35 was similar to that of other retromer subunits, as demonstrated by colocalization with endogenous hVps26 (Fig. 2, J–L). The YFP-hVps35 puncta were often adjacent to dark vacuoles that probably correspond to the vacuolar part of endosomes observed by EM (Fig. 6 A). Both the fluorescent and dark structures remained tightly associated as they moved together in the cytoplasm over time (Fig. 6 A; Video 1, available at http://www.jcb.org/cgi/content/full/jcb.200312055/DC1). The YFP-hVps35 puncta often gave rise to long fluorescent tubules that extended in various directions, some toward the juxtanuclear area of the cell and others toward other puncta (Fig. 6 A; Video 1). Treatment with the microtubule-depolymerizing agent nocodazole prevented the formation of tubules (unpublished data). FRAP of the YFP-hVps35 puncta showed that this protein reassociated with the same puncta with a half-time of 6.5 $\pm$ 0.4 s (Fig. 6, B and C). These results confirmed and extended the observations on fixed cells by demonstrating that YFP-hVps35 is dynamically associated with structures adjacent to vacuolar profiles from which tubules arise.

Inhibition of retromer expression by siRNA increases lysosomal turnover of the CI-MPR

Next, we sought to establish a functional connection between retromer and the CI-MPR by depleting cells of hVps26 using a specific small interfering RNA (siRNA). After 72 h of treatment with this siRNA, the levels of hVps26 decreased, as observed by both immunofluorescence microscopy (Fig. 7, A and B) and immunoblotting (Fig. 7 I). Quantification of the corresponding immunoblots showed that the amount of hVps26 decreased by 90 $\pm$ 5% ($n = 6$). The levels of the other retromer subunits were affected by the hVps26 depletion to different extents, with hVps29 and hVps35 levels being substantially decreased and Snx1 and Snx2 levels being largely unaltered (Fig. 7 I).

The depletion of hVps26 had no effect on the steady-state distribution or levels of various transmembrane proteins including TGN46, the TfR, Lamp-1, and the EGF receptor (Fig. 7, C–F, I, and unpublished data). It also had no apparent effect on TfR internalization and recycling, as well as on internalization and degradation of the EGF receptor, as assessed by fluorescence microscopy (Fig. S1, available at http://www.jcb.org/cgi/content/full/jcb.200312055/DC1). However, the levels of CI-MPR were significantly reduced (to 38 $\pm$ 21%; $n = 8$) in cells depleted of hVps26, as observed by both immunofluorescence microscopy (Fig. 7, G and H) and immunoblot analysis (Fig. 7 I). The remaining CI-MPR exhibited a more dispersed distribution in the cytoplasm, suggesting a shift towards endosomes (Fig. 7 H). Similar results were obtained by siRNA-mediated depletion of hVps35 (Fig. S2). We reasoned that the reduction in CI-MPR levels could be due to degradation of the receptor. To test this hypothesis, we performed a cycloheximide chase experiment in which the levels of CI-MPR in mock- and siRNA-treated cells were examined at different times after inhibition of protein synthesis (Fig. 8 A). In mock-treated cells, the receptor had a half-life of 27 h (Fig. 8 A; Fig. S3), which was similar to that previously reported by Creek and Sly (1983). In contrast, in the siRNA-treated cells, the half-life of the CI-MPR was reduced to 7 h (Fig. 8 A; Fig. S3; half-lives are the mean from three determinations). To determine whether this degradation occurred in lysosomes, we

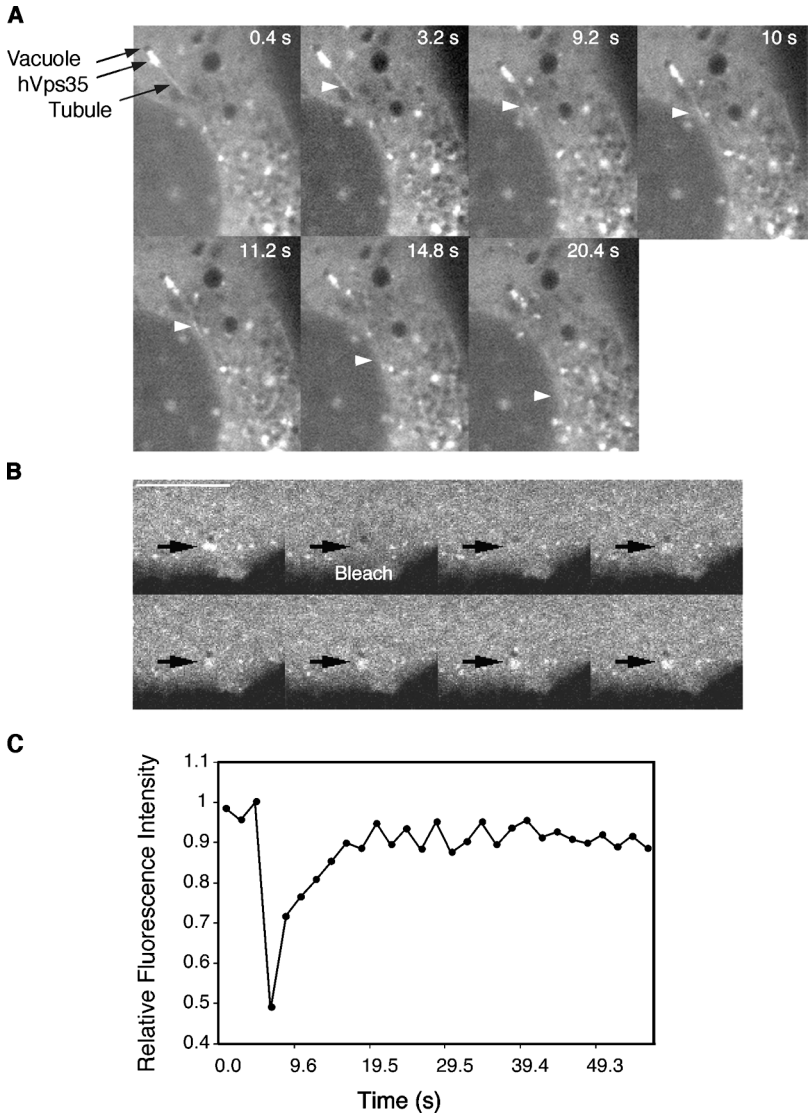

Figure 6. **Fluorescence imaging of YFP-hVps35 in live cells.** (A) Live M1 cells stably expressing YFP-hVps35 were imaged by confocal microscopy at 37°C. Notice the presence of YFP-hVps35 in punctate and tubular structures that are often associated with dark vacuolar profiles. The tubule marked by the arrowhead extends and detaches from a vacuole, and then heads toward the juxtanuclear area. The dark vacuole moves along with the YFP-hVps35–positive structure. The times at which each image was collected are indicated. (B) M1 cells stably expressing YFP-hVps35 were pretreated with 10 μM nocodazole for 1 h at 37°C before FRAP. 100% power in the 488-nm line was applied for photobleaching in the region indicated by the arrow. Recovery was monitored over time. The sequence shown represents frames taken every 2 s. Bar, 10 μm. (C) Quantification of the data in B shows recovery with a half-time of 6.5 s.

incubated the siRNA-treated cells with the lysosomal inhibitors leupeptin and E64, plus or minus methionine methyl ester. We observed that these treatments prevented the decrease of CI-MPR levels (Fig. 8 B) and resulted in the accumulation of the CI-MPR in large vesicles (Fig. 8, C–H) that contained Lamp-1-YFP (Fig. 8, I–K). Together, these observations indicate that the absence of retromer causes increased delivery of the CI-MPR to lysosomes.

Finally, we assessed the consequences of CI-MPR degradation on lysosomal function. The activities of β-hexosaminidase and β-glucuronidase, which are normally sorted to lysosomes by the MPRs, were reproducibly decreased by 25% in extracts of cells treated for 72 h with a single dose of hVps26 siRNA (Fig. 9 A). In contrast, aconitase activity, which is present in the cytosol and mitochondria, was not affected by depletion of hVps26 (Fig. 9 A). This indicated that the reductions of lysosome hydrolase activities were specific. Treatment with two doses of hVps26 siRNA at 72-h intervals (for a total of 144 h) resulted in significant loss of viability, which precluded accurate measurement of lysosomal enzyme activities. However, the cells that remained attached to the cover glasses exhibited reduced staining for cathepsin D (Fig. 9, B and C), another enzyme sorted by the MPRs. In addition, we noticed swelling of the lysosomes stained for Lamp-1 in the hVps26 siRNA-treated cells (Fig. 9, D and E), which probably resulted from accumulation of undegraded materials in lysosomes.

Discussion

The results presented here support a role for the mammalian retromer in the retrieval of the CI-MPR from endosomes to the TGN. This role appears to involve the recognition of a bipartite determinant in the cytosolic domain of the CI-MPR (residues 48–100) by the hVps35 subunit of retromer. The retromer-binding determinant does not overlap with the YSKV signal involved in CI-MPR endocytosis (Jadot et al., 1992) or the acidic cluster–dileucine signal responsible for sorting of the receptor from the TGN to endosomes (Johnson and Kornfeld, 1992; Chen et al., 1993, 1997). In addition, the retromer-binding determinant differs from those sorting signals in that it is much longer and contains many critical residues, perhaps indicating that it is conformational in nature. We have been unable to demonstrate a

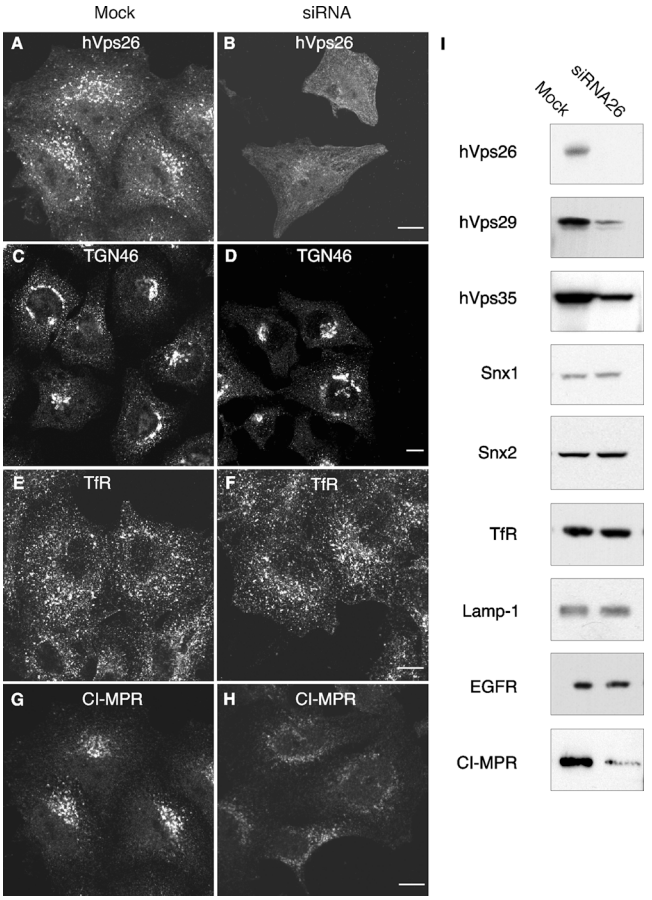

Figure 7. **Effect of RNA-mediated interference of hVps26 on the expression of retromer subunits.** HeLa cells were either mock treated or treated with hVps26 siRNA (siRNA) for 72 h, and were then analyzed by immunofluorescence microscopy (A–H) and immunoblotting (I). Immunofluorescence microscopy was performed with antibodies directed to endogenous hVps26 (A and B), TGN46 (C and D), TfR (E and F), or CI-MPR (G and H), all followed by the corresponding secondary antibodies labeled with either Alexa® 488 or Cy3. Bars, 10 μm. Immunoblots were probed with antibodies to the proteins indicated in I and are described in more detail in the Materials and methods.

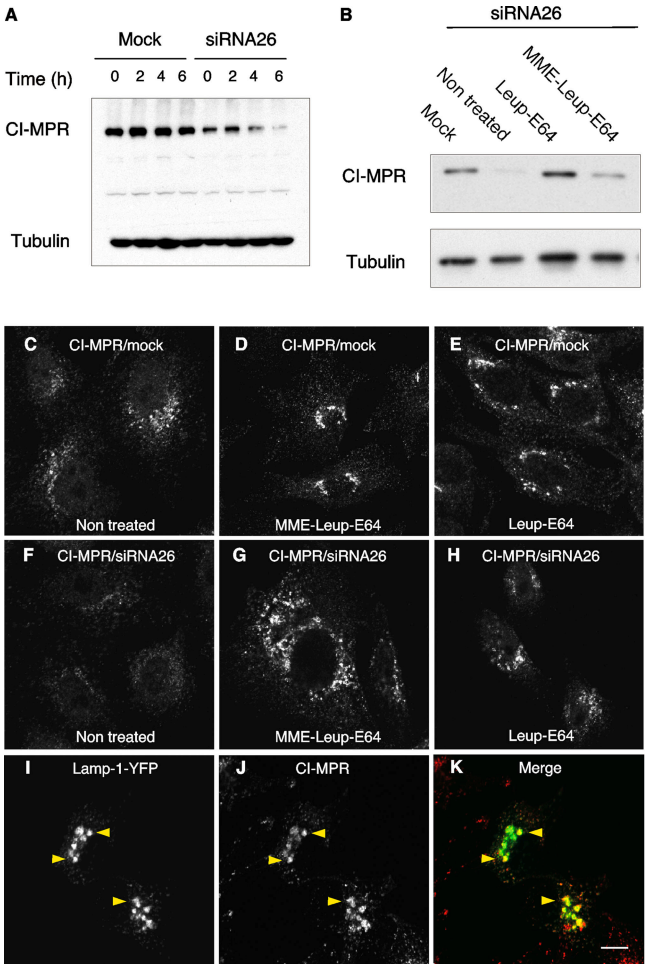

Figure 8. **Lysosomal degradation of the CI-MPR upon depletion of retromer.** (A) Immunoblot analysis of CI-MPR half-life in mock- and hVps26-siRNA–treated HeLa cells after treatment with 40 μg/ml cycloheximide. Tubulin was used as a control. (B) Immunoblot analysis of CI-MPR levels after silencing hVps26. HeLa cells were incubated in the absence or presence of the lysosomal inhibitors leupeptin (Leup, 1 mg/ml), E64 (5 μg/ml), and methionine methyl ester (MME, 10 mM) for 3 h, as indicated in the figure. Blots were probed with antibodies to the CI-MPR or tubulin (control). (C–K) Immunofluorescence microscopy of mock-treated (C–E) or hVps26-siRNA–treated HeLa cells (F–K) incubated in the absence or presence of the lysosomal inhibitors described in A, and stained with the antibody to the CI-MPR and donkey Cy3-conjugated anti–mouse Igs. Lamp-1-YFP (I–K) was expressed by transient transfection. In this case, hVps26-depleted cells were treated with MME/Leup/E64 protease inhibitors. Arrowheads in I–K indicate colocalization of Lamp-1-YFP with CI-MPR. Bar, 10 μm.

similar interaction with the cytosolic domain of the CD-MPR, but we did detect an interaction with the cytosolic domain of metallocarboxypeptidase D (unpublished data), a transmembrane protein that cycles between the TGN and the plasma membrane (Varlamov and Fricker, 1998).

The hVps35–CI-MPR interactions are likely physiological because human retromer partially colocalizes with a pool of CI-MPR in vesicular–tubular structures distributed throughout the cytoplasm, though less so with a pericentriolar pool of CI-MPR. The morphology and composition of the structures where retromer colocalizes with CI-MPR correspond to those of early endosomes (Geuze et al., 1983; Hopkins, 1983; Griffiths et al., 1989; Ludwig et al., 1991) or intermediates in the maturation of early to late endosomes (Geuze et al., 1983; Hirst et al., 1998; Raiborg et al., 2002, 2003; Sachse et al., 2002). Many of these endosomes have electron-dense deposits resembling the previously described bilayered clathrin- and Hrs-containing coats (Raposo et al., 2001; Raiborg et al., 2002, 2003; Sachse et al., 2002). They contain the TfR and are enlarged by expression of Rab5Q79L, but also enclose numerous intraluminal vesicles. All of these are well-established characteristics of the bilayered coated endosomes, which represent a transition from early to late endosomal stages (Raposo et al., 2001; Raiborg et al., 2002, 2003; Sachse et al., 2002). Retromer is most concentrated on tubules that radiate from the vacuolar aspect of these endosomes, whereas CI-MPR appears evenly distributed between the radiating tubules and intraluminal vesicles. These observations indicate that a function of retromer may be to extract CI-MPR from endosomes—perhaps even from the intraluminal vesicles—through capture

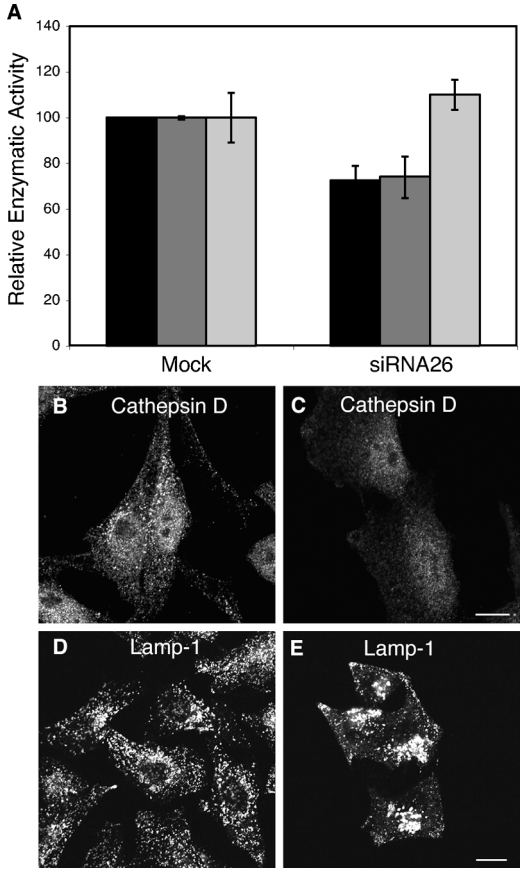

Figure 9. **Lysosomal alterations in retromer-depleted cells.** (A) Quantification of β-glucuronidase (black bars), β-hexosaminidase (dark gray bars), and aconitase (light gray bars) activities in lysates from mock-treated and hVps26-depleted HeLa cells. The results are expressed as the mean ± SD of at least three experiments, each of which was performed in triplicate. (B) Immunofluorescence microscopy of mock-treated (B and D) and hVps26-siRNA–treated (C and E) cells stained with an antibody to cathepsin D and donkey Alexa® 488–conjugated anti–rabbit Igs (B and C), or an antibody to Lamp-1 and donkey Cy3-conjugated anti–mouse Igs (D and E). Bars, 10 μm.

into a recycling tubular compartment. Although the tubules themselves appear mobile, it is at present unclear whether they constitute the actual transport carriers or give rise to vesicular transport intermediates. The association of retromer with tubules is consistent with the presence in Snx1 and Snx2 of a BAR-like domain that has the ability to sense highly curved membranes (Peter et al., 2004).

The involvement of retromer in recycling of CI-MPR to the TGN is further supported by the phenotype elicited by siRNA-mediated interference of retromer expression. This treatment resulted in enhanced lysosomal degradation of CI-MPR and, consequently, decreased steady-state levels of this receptor. Cellular levels of lysosomal hydrolases also decreased and lysosomes swelled, probably due to accumulation of undegraded materials within their lumen. The most logical interpretation of these observations is that retromer keeps the CI-MPR from going to lysosomes by mediating its removal from maturing endosomes. We think that the CI-MPR determinant recognized by retromer might encompass a "lysosomal avoidance" signal functionally similar to that described by Kornfeld and colleagues in the cytosolic domain of the CD-MPR (Rohrer et al., 1995). However, the phenylalanine–tryptophan motif that defines this signal in the CD-MPR (Rohrer et al., 1995) is not present in the CI-MPR, indicating that the latter must be structurally different. It is noteworthy that delivery to lysosomes is the fate of the CI-MPR in the absence of retromer. This indicates that other determinants within the CI-MPR direct its targeting to lysosomes in the absence of retromer. These determinants may be responsible for inclusion of the CI-MPR into intraluminal vesicles bound for destruction in lysosomes. In this regard, the luminal domain of the CI-MPR has been shown to detain chimeric proteins in endosomes (Dintzis et al., 1994), although we do not know if this property contributes to the lysosomal degradation of the receptor in the absence of retromer.

There is a general consensus that the CI-MPR and its cargo hydrolases follow an intracellular route from the TGN to the endosomal–lysosomal system (Kornfeld and Mellman, 1989; Ghosh et al., 2003). However, the initial port of entry into this system remains a matter of debate. Indeed, different reports have presented evidence for transport from the TGN to either early or late endosomes (Geuze et al., 1985; Bock et al., 1997; Ludwig et al., 1991; Runquist and Havel, 1991; Rijnboutt et al., 1992; Hirst et al., 1998; Klumperman et al., 1998; Press et al., 1998; Meyer et al., 2001; Waguri et al., 2003). Although our experiments do not directly address this issue, they highlight the critical importance of passage through early endosomes or early–late endosomal intermediates in the biosynthetic or endocytic trafficking of the CI-MPR, as previously proposed (Ludwig et al., 1991; Runquist and Havel, 1991; Rijnboutt et al., 1992; Hirst et al., 1998; Lin et al., 2004). Because dissociation of the lysosomal hydrolases from both the CI-MPR and CD-MPR occurs between pH 5.0 and 6.0 (Sahagian et al., 1981; Hoflack and Kornfeld, 1985), some maturation of the early endosomes must take place before the retromer can assume its role in the retrieval of the unoccupied receptors.

The above considerations notwithstanding, our results do not rule out that the CI-MPR–hydrolase complexes may be delivered in part to late endosomes (i.e., those lacking TfR but containing Lamps). It is indeed possible that more than one endosomal compartment acts as the acceptor for TGN-derived carriers, or that some CI-MPR traffics from early to late endosomes prior to retrieval. Proteins such as AP-1 (Meyer et al., 2000, 2001), TIP47 (Diaz and Pfeffer, 1998; Orsel et al., 2000; Krise et al., 2000), and PACS-1 (Wan et al., 1998) could cooperate with retromer in CI-MPR recycling from early endosomes, perhaps by participating in consecutive sorting steps along the route to the TGN, or they could be involved in CI-MPR recycling from late endosomes, as previously proposed for TIP47 (Diaz and Pfeffer, 1998; Barbero et al., 2002). The existence of distinct TGN retrieval pathways originating from early and late endosomes is well established in both mammalian (Mallet and Maxfield, 1999) and yeast (Hettema et al., 2003) cells.

The alterations in lysosomal/vacuolar sorting resulting from depletion of retromer in mammalian cells (this paper) and yeast cells (Seaman et al., 1998) are remarkably similar, demonstrating the conservation of this aspect of the protein-sorting machinery. However, a review of the published work on the mammalian Snx1 and Snx2 makes our results surpris-

ing. Snx1 and Snx2 have been shown to interact with the cytosolic domains of the EGF, transferrin, and leptin receptors, and of protease-activated receptor-1 (Kurten et al., 1996; Haft et al., 1998; Wang et al., 2002). In the case of the EGF receptor, interaction with Snx1 is thought to enhance its degradation in lysosomes (Kurten et al., 1996), contrary to the role of retromer in CI-MPR trafficking (this paper). A possible explanation for this difference could be that Snx1 and Snx2 are not only components of retromer, but also are subunits of other still undefined complexes involved in targeting to late endosomes and lysosomes. Resolving this issue will require a more detailed analysis of the diversity of retromer subunit assembly and function.

Materials and methods

Recombinant constructs

Full-length and truncated hVps35 constructs were made by PCR and subcloned in pLexA as described previously (Haft et al., 2000). The CI-MPR cytosolic domain (last 164 amino acids) as well as truncation mutants of this domain (constructed using the QuikChange® kit; Stratagene) were subcloned into the EcoR1–Xho1 sites of the pB42AD vector. Myc-Snx2 in pCDNA(3.1±) (Invitrogen) was described previously (Haft et al., 2000). Xho1 and BamH1 sites were added to the 5′ and 3′ ends, respectively, of full-length hVps35 by PCR and subcloned into the corresponding site in pEYFP-C1 (CLONTECH Laboratories, Inc.). Lamp-1-YFP in pEYFP-N2 was a gift from George Patterson (National Institutes of Health, Bethesda, MD).

Yeast two-hybrid assays

The MATCHMAKER pLexA system was used (CLONTECH Laboratories, Inc.). Plasmid transformation of the EGY48[p8op-lacZ] strain was by the lithium acetate method. Co-transformants were selected using SD medium −Ura/−Trp/−His (−2/−Ura plates); individual colonies were picked and resuspended in water to a final OD_{600} of 0.1. Finally, 5 μl of this suspension was plated in parallel on −2/−Ura plates and SD-Gal/Raf −Ura/−Trp/−His/−Leu (−3/−Ura plates). Growth was checked after 72 h at 30°C. Lamin C in pB42AD was used as a negative control.

Cell transfection

Human HeLa or M1 fibroblast cells (American Type Culture Collection, Manassas, VA) were cultured on 6-well plates at 37°C in DME/high glucose (Biosource International) supplemented with 10% (vol/vol) FBS, 100 U/ml penicillin, and 100 μg/ml streptomycin. When cells reached 60% confluency, they were transfected with 1 μg DNA constructs using the FuGENE™ reagent (Roche) according to the manufacturer's instructions. For stable expression of YFP-hVps35 in M1 cells, cells were transfected and grown in medium containing 0.5 mg/ml G418 (Geneticin; GIBCO BRL) as the selective agent. Positive clones were analyzed for expression of YFP-hVps35 by fluorescence microscopy.

RNA interference

The sequences 5′-CTCTATTAAGATGGAAGTG-3′ and 5′-ATTTGGTGCGCCTCAGTCA-3′ were selected as targets for silencing hVps26 and hVps35 expression, respectively, with siRNA. Transfection of HeLa cells with hVps26 or hVps35 siRNA (Dharmacon) was performed using Oligofectamine™ (Invitrogen) following the manufacturer's protocol. Cells were analyzed after 72 h or after two consecutive transfections at 72-h intervals.

Antibodies and immunofluorescence microscopy

Immunofluorescence microscopy was performed as described previously (Caplan et al., 2002). mAbs used were as follows: 9E10 to the myc epitope (BabCo); 2G11 to the CI-MPR (Research Diagnostics); B3/25 to the TfR (Boehringer); and H4A3 to Lamp-1 (Developmental Studies Hybridoma Bank, Iowa City, IO). The rabbit pAbs to the human retromer proteins hVps26, hVps29, hVps35, Snx1, and Snx2 have been described previously (Haft et al., 2000). Other pAbs used were sheep antibody to human TGN46 (Serotec) and rabbit antibody to cathepsin D (Upstate Biotechnology). Donkey Cy3-conjugated AffiniPure anti–mouse Igs (Jackson ImmunoResearch Laboratories) and donkey Alexa® 488–conjugated anti–rabbit Igs (Molecular Probes, Inc.) were used as secondary antibodies. For wortmannin treatment, cells were incubated in complete DME containing 100 nM wortmannin (Sigma-Aldrich) for 30 min at 37°C. Fluorescently labeled cells were examined using an inverted confocal laser scanning microscope (model LSM 510; Carl Zeiss MicroImaging, Inc.) equipped with argon, HeNe, and krypton lasers, and a 63Å 1.4 NA objective. Alexa® 488 and Cy3 fluorescence was visualized using excitation filters at 488 and 543 nm and emission filters at 505–530 and 560 nm, respectively.

Electron microscopy

HeLa cells were fixed with 4% formaldehyde and 0.2% glutaraldehyde, and were then processed for ultrathin frozen sectioning as described previously (Dell'Angelica et al., 2000). The mAb H68.4 to the TfR was obtained from Zymed Laboratories, and the mAb 2G11 to the CI-MPR was a gift from Suzanne Pfeffer (Stanford University, Stanford, CA). All other antibodies used have been mentioned above. The protein A–gold used to visualize the presence of antibody in the electron microscope was obtained from the University of Utrecht (Utrecht, Netherlands).

Live-cell imaging

Stably transfected YFP-hVps35 M1 cells were grown on LabTek™ chambers (Nunc) and transferred into culture medium buffered with 25 mM Hepes/KOH, pH 7.4. Experiments were performed on a spinning disk confocal microscope (Ultraview LCI Confocal scanner; PerkinElmer) equipped with a stage heated to 37°C, and a 63Å 1.4 NA objective. YFP-hVps35 was excited with a 488-nm line and imaged through a 500 LP emission filter. FRAP experiments were performed with an inverted confocal laser scanning microscope (model LSM 510; Carl Zeiss MicroImaging, Inc.). Cells were pretreated with 10 μM nocodazole for 1 h at 37°C before recording. 100% power in the 488-nm line was applied for photobleaching. Images were collected using a 505–530-nm emission filter. Data were processed to QuickTime format in NIH Image 1.3 software.

Immunoblotting

Antisera dilutions used for immunoblotting were as follows: 1:1,000 for rabbit anti-hVps35, -hVps29, and -hVps26; 1:2,000 for rabbit anti-Snx1 and -Snx2; 1:200 for rabbit antibody to the cytosolic domain of CI-MPR (a gift of Thomas Braulke, University of Hamburg, Hamburg, Germany); 1:1,000 for mouse anti α-tubulin (DM1A; Sigma-Aldrich); 1:1,000 for mouse H4A3 anti-Lamp-1; and 1:500 for rabbit anti-EGF receptor (sc-03; Santa Cruz Biotechnology, Inc.). Immunoblots were developed using HRP-coupled secondary antisera and an ECL reagent (Western Lightning™; PerkinElmer).

Treatment with lysosomal inhibitors

Mock- and siRNA-treated cells were incubated for 3 h at 37°C in complete DME containing 1 mg/ml leupeptin (Roche) and 5 μg/ml E64 (Sigma-Aldrich) plus or minus 10 mM methionine methyl ester (Sigma-Aldrich). Cells were scraped, lysed, and analyzed by SDS-PAGE (6% acrylamide or 4–20% acrylamide gradient) and immunoblotting. In addition, coverslips were fixed and analyzed by immunofluorescence microscopy.

Measurements of enzyme activity

Crude cell lysates were prepared by centrifugation of HeLa cells for 10 min at 2,000 *g*. The cell pellet was resuspended in 50 mM Tris-HCl, pH 7.4, 1% (wt/vol) Triton X-100, 300 mM NaCl, 5 mM EDTA, and protease inhibitors, and was incubated on ice for 30 min. Complete lysis was achieved by 10 passages through a 20-gauge needle. The sample was then centrifuged for 15 min at 16,000 *g*. Protein was quantified by the BCA assay (Pierce Chemical Co.) using BSA as a standard. β-glucuronidase and β-hexosaminidase activities were measured using 5 mM 4-methylumbelliferyl-β-D-glucuronide and 10 mM 4-methylumbelliferyl-2-acetamido-2-deoxy-β-D-glucopiranoside (Sigma-Aldrich) as substrates, respectively (Nolan, 1992). Fluorescence spectra were acquired on a fluorimeter (FluoroMax-3; Jobin Yvon), setting excitation wavelength at 360 nm and emission and excitation slits between 1 and 1.5 nm. Fluorescence intensity at 445 nm was recorded. Aconitase activity was measured in cell lysates prepared in the presence of citrate as described by Meyron-Holtz et al. (2004).

Cycloheximide chase

Mock- and siRNA-treated cells were trypsinized and incubated in suspension at 37°C in complete DME containing 25 mM Hepes buffer, pH 7.4, and 40 μg/ml cycloheximide (Sigma-Aldrich). At the corresponding time point, cells were spun for 10 min at 2,000 *g*, lysed as described above, and analyzed by SDS-PAGE and immunoblotting.

Online supplemental material

Video 1 shows stably transfected YFP-hVps35 M1 cells grown on LabTek™ chambers (Nunc) and transferred into culture medium buffered with

25 mM Hepes/KOH, pH 7.4. Experiments were performed on a spinning disk microscope (Ultraview LCI Confocal scanner; PerkinElmer) equipped with a stage heated to 37°C, and a 63Å 1.4 NA objective. YFP-hVps35 was excited with a 488-nm line and imaged through a 500 LP emission filter. Fig. S1 shows that the trafficking of the TfR and the EGF receptor is not affected by retromer depletion. Fig. S2 shows the effects of siRNA-mediated depletion of hVps35 on the distribution and levels of the CI-MPR. Fig. S3 shows a representation of the kinetics of CI-MPR turnover. Online supplemental material available at http://www.jcb.org/cgi/content/full/jcb.200312055/DC1.

We thank Xiaolin Zhu and Anitza San Miguel for expert technical assistance. We are also grateful to Suzanne Pfeffer, Thomas Braulke, and George Patterson for gifts or reagents, and to Rafael Mattera for critical review of the manuscript.

Cecilia Arighi is the recipient of a postdoctoral fellowship from Pew Charitable Trust.

Submitted: 8 December 2003
Accepted: 5 March 2004

References

Barbero, P., L. Bittova, and S.R. Pfeffer. 2002. Visualization of Rab9-mediated vesicle transport from endosomes to the trans-Golgi in living cells. *J. Cell Biol.* 156:511–518.

Bock, J.B., J. Klumperman, S. Davanger, and R.H. Scheller. 1997. Syntaxin 6 functions in trans-Golgi network vesicle trafficking. *Mol. Biol. Cell.* 8:1261–1271.

Caplan, S., N. Naslavsky, L.M. Hartnell, R. Lodge, R.S. Polishchuk, J.G. Donaldson, and J.S. Bonifacino. 2002. A tubular EHD1-containing compartment involved in the recycling of major histocompatibility complex class I molecules to the plasma membrane. *EMBO J.* 21:2557–2567.

Chen, H.J., J. Remmler, J.C. Delaney, D.J. Messner, and P. Lobel. 1993. Mutational analysis of the cation-independent mannose 6-phosphate/insulin-like growth factor II receptor. A consensus casein kinase II site followed by 2 leucines near the carboxyl terminus is important for intracellular targeting of lysosomal enzymes. *J. Biol. Chem.* 268:22338–22346.

Chen, H.J., J. Yuan, and P. Lobel. 1997. Systematic mutational analysis of the cation-independent mannose 6-phosphate/insulin-like growth factor II receptor cytoplasmic domain. An acidic cluster containing a key aspartate is important for function in lysosomal enzyme sorting. *J. Biol. Chem.* 272:7003–7012.

Cooper, A.A., and T.H. Stevens. 1996. Vps10p cycles between the late-Golgi and prevacuolar compartments in its function as the sorting receptor for multiple yeast vacuolar hydrolases. *J. Cell Biol.* 133:529–542.

Costaguta, G., C.J. Stefan, E.S. Bensen, S.D. Emr, and G.S. Payne. 2001. Yeast Gga coat proteins function with clathrin in Golgi to endosome transport. *Mol. Biol. Cell.* 12:1885–1896.

Creek, K.E., and W.S. Sly. 1983. Biosynthesis and turnover of the phosphomannosyl receptor in human fibroblasts. *Biochem. J.* 214:353–360.

Dell'Angelica, E.C., R. Puertollano, C. Mullins, R.C. Aguilar, J.D. Vargas, L.M. Hartnell, and J.S. Bonifacino. 2000. GGAs: a family of ADP ribosylation factor-binding proteins related to adaptors and associated with the Golgi complex. *J. Cell Biol.* 149:81–94.

Deloche, O., B.G. Yeung, G.S. Payne, and R. Schekman. 2001. Vps10p transport from the trans-Golgi network to the endosome is mediated by clathrin-coated vesicles. *Mol. Biol. Cell.* 12:475–485.

Diaz, E., and S.R. Pfeffer. 1998. TIP47: a cargo selection device for mannose 6-phosphate receptor trafficking. *Cell.* 93:433–443.

Dintzis, S.M., V.E. Velculescu, and S.R. Pfeffer. 1994. Receptor extracellular domains may contain trafficking information. Studies of the 300-kDa mannose 6-phosphate receptor. *J. Biol. Chem.* 269:12159–12166.

Doray, B., P. Ghosh, J. Griffith, H.J. Geuze, and S. Kornfeld. 2002. Cooperation of GGAs and AP-1 in packaging MPRs at the trans-Golgi Network. *Science.* 297:1700–1703.

Geuze, H.J., J.W. Slot, G.J. Strous, and A.L. Schwartz. 1983. The pathway of the asialoglycoprotein-ligand during receptor-mediated endocytosis: a morphological study with colloidal gold/ligand in the human hepatoma cell line, Hep G2. *Eur. J. Cell Biol.* 32:38–44.

Geuze, H.J., J.W. Slot, G.J. Strous, A. Hasilik, and K. von Figura. 1985. Possible pathways for lysosomal enzyme delivery. *J. Cell Biol.* 101:2253–2262.

Geuze, H.J., W. Stoorvogel, G.J. Strous, J.W. Slot, J.E. Bleekemolen, and I. Mellman. 1988. Sorting of mannose 6-phosphate receptors and lysosomal membrane proteins in endocytic vesicles. *J. Cell Biol.* 107:2491–2501.

Ghosh, P., N.M. Dahms, and S. Kornfeld. 2003. Mannose 6-phosphate receptors: new twists in the tale. *Nat. Rev. Mol. Cell Biol.* 4:202–212.

Glickman, J.N., E. Conibear, and B.M. Pearse. 1989. Specificity of binding of clathrin adaptors to signals on the mannose-6-phosphate/insulin-like growth factor II receptor. *EMBO J.* 8:1041–1047.

Griffiths, G., R. Back, and M. Marsh. 1989. A quantitative analysis of the endocytic pathway in baby hamster kidney cells. *J. Cell Biol.* 109:2703–2720.

Haft, C.R., M.L. Sierra, V.A. Barr, T.H. Haft, and S.I. Taylor. 1998. Identification of a family of sorting nexin molecules and characterization of their association with receptors. *Mol. Cell. Biol.* 18:7278–7287.

Haft, C.R., M.L. Sierra, R. Bafford, M.A. Lesniak, V.A. Barr, and S.I. Taylor. 2000. Human orthologs of yeast vacuolar protein sorting proteins Vps26, Vps29, and Vps35: assembly into multimeric complexes. *Mol. Biol. Cell.* 11:4105–4116.

Hettema, E.H., M.J. Lewis, M.W. Black, and H.R. Pelham. 2003. Retromer and the sorting nexins Snx4/41/42 mediate distinct retrieval pathways from yeast endosomes. *EMBO J.* 22:548–557.

Hirst, J., C.E. Futter, and C.R. Hopkins. 1998. The kinetics of mannose 6-phosphate receptor trafficking in the endocytic pathway in HEp-2 cells: the receptor enters and rapidly leaves multivesicular endosomes without accumulating in a prelysosomal compartment. *Mol. Biol. Cell.* 9:809–816.

Hirst, J., W.W.Y. Lui, N.A. Bright, N. Totty, M.N.J. Seaman, and M.S. Robinson. 2000. A family of proteins with γ-adaptin and VHS domains that facilitate trafficking between the TGN and the vacuole/lysosome. *J. Cell Biol.* 149:67–79.

Hirst, J., M.R. Lindsay, and M.S. Robinson. 2001. Golgi-localized, γ-ear-containing, ADP-ribosylation factor-binding proteins: roles of the different domains and comparison with AP-1 and clathrin. *Mol. Biol. Cell.* 12:3573–3588.

Hoflack, B., and S. Kornfeld. 1985. Purification and characterization of a cation-dependent mannose 6-phosphate receptor from murine P388D1 macrophages and bovine liver. *J. Biol. Chem.* 260:12008–12014.

Honing, S., M. Sosa, A. Hille-Rehfeld, and K. von Figura. 1997. The 46-kDa mannose 6-phosphate receptor contains multiple binding sites for clathrin adaptor. *J. Biol. Chem.* 272:19884–19890.

Hopkins, C.R. 1983. Intracellular routing of transferrin and transferrin receptors in epidermoid carcinoma A431 cells. *Cell.* 35:321–330.

Horazdovsky, B.F., B.A. Davies, M.N. Seaman, S.A. McLaughlin, S. Yoon, and S.D. Emr. 1997. A sorting nexin-1 homologue, Vps5p, forms a complex with Vps17p and is required for recycling the vacuolar protein-sorting receptor. *Mol. Biol. Cell.* 8:1529–1541.

Jadot, M., W.M. Canfield, W. Gregory, and S. Kornfeld. 1992. Characterization of the signal for rapid internalization of the bovine mannose 6-phosphate/insulin-like growth factor-II receptor. *J. Biol. Chem.* 267:11069–11077.

Johnson, K.F., and S. Kornfeld. 1992. The cytoplasmic tail of the mannose 6-phosphate/insulin-like growth factor-II receptor has two signals for lysosomal enzyme sorting in the Golgi. *J. Cell Biol.* 119:249–257.

Klumperman, J., A. Hille, T. Veenendaal, V. Oorschot, W. Stoorvogel, K. von Figura, and H.J. Geuze. 1993. Differences in the endosomal distributions of the two mannose 6-phosphate receptors. *J. Cell Biol.* 121:997–1010.

Klumperman, J., R. Kuliawat, J.M. Griffith, H.J. Geuze, and P. Arvan. 1998. Mannose 6-phosphate receptors are sorted from immature secretory granules via adaptor protein AP-1, clathrin, and syntaxin 6-positive vesicles. *J. Cell Biol.* 141:359–371.

Kornfeld, S., and I. Mellman. 1989. The biogenesis of lysosomes. *Annu. Rev. Cell Biol.* 5:483–525.

Krise, J.P., P.M. Sincock, J.G. Orsel, and S.R. Pfeffer. 2000. Quantitative analysis of TIP47-receptor cytoplasmic domain interactions. Implication for endosome-to-trans Golgi network trafficking. *J. Biol. Chem.* 275:25188–25193.

Kurten, R.C., D.L. Cadena, and G.N. Gill. 1996. Enhanced degradation of EGF receptors by a sorting nexin, SNX1. *Science.* 272:1008–1010.

Kurten, R.C., A.D. Eddington, P. Chowdhury, R.D. Smith, A.D. Davidson, and B.B. Shank. 2001. Self-assembly and binding of a sorting nexin to sorting endosomes. *J. Cell Sci.* 114:1743–1756.

Lin, S.X., W.G. Mallet, A.Y. Huang, and F.R. Maxfield. 2004. Endocytosed cation-independent mannose 6-phosphate receptor traffics via the endocytic recycling compartment en route to the trans-Golgi network and a subpopulation of late endosomes. *Mol. Biol. Cell.* 15:721–733.

Ludwig, T., G. Griffiths, and B. Hoflack. 1991. Distribution of newly synthesized lysosomal enzymes in the endocytic pathway of normal rat kidney cells. *J. Cell Biol.* 115:1561–1572.

Mallet, W.G., and F.R. Maxfield. 1999. Chimeric forms of furin and TGN38 are

transported with the plasma membrane in the trans-Golgi network via distinct endosomal pathways. *J. Cell Biol.* 146:345–359.

Marcusson, E.G., B.F. Horazdovsky, J.L. Cereghino, E. Gharakhanian, and S.D. Emr. 1994. The sorting receptor for carboxypeptidase Y is encoded by the VPS10 gene. *Cell.* 77:579–586.

Mauxion, F., R. Le Borgne, H. Munier-Lehmann, and B.A. Hoflack. 1996. A casein kinase II phosphorylation site in the cytoplasmic domain of the cation-dependent mannose 6-phosphate receptor determines the high affinity interaction of the AP-1 Golgi assembly proteins with membranes. *J. Biol. Chem.* 271:2171–2178.

Meyer, C., D. Zizioli, S. Lausmann, E.L. Eskelinen, J. Hamann, P. Saftig, K. von Figura, and P. Schu. 2000. μ1A-adaptin-deficient mice: lethality, loss of AP-1 binding and rerouting of mannose 6-phosphate receptors. *EMBO J.* 19:2193–2203.

Meyer, C., E.L. Eskelinen, M.R. Guruprasad, K. von Figura, and P. Schu. 2001. μ1A deficiency induces a profound increase in MPR300/IGF-II receptor internalization rate. *J. Cell Sci.* 114:4469–4476.

Meyron-Holtz, E.G., M.C. Ghosh, K. Iwai, T. LaVaute, X. Brazzolotto, U.V. Berger, W. Land, H. Ollivierre-Wilson, A. Grinberg, P. Love, and T.A. Rouault. 2004. Genetic ablations of iron regulatory proteins 1 and 2 reveal why iron regulatory protein 2 dominates iron homeostasis. *EMBO J.* 23: 386–395.

Mullins, C., and J.S. Bonifacino. 2001. Structural requirements for function of yeast GGAs in vacuolar protein sorting, α-factor maturation, and interactions with clathrin. *Mol. Cell. Biol.* 21:7981–7994.

Nolan, C. 1992. Receptor-mediated endocytosis and lysosomal transport. *In* Protein Targeting: A Practical Approach. Oxford University Press, Oxford, UK. Section 1.6.

Nothwehr, S.F., P. Bruinsma, and L.S. Strawn. 1999. Distinct domains within Vps35p mediate the retrieval of two different cargo proteins from the yeast prevacuolar/endosomal compartment. *Mol. Biol. Cell.* 10:875–890.

Nothwehr, S.F., S.A. Ha, and P. Bruinsma. 2000. Sorting of yeast membrane proteins into an endosome-to-Golgi pathway involves direct interaction of their cytosolic domains with Vps35p. *J. Cell Biol.* 151:297–310.

Orsel, J.G., P.M. Sincock, J.P. Krise, and S.R. Pfeffer. 2000. Recognition of the 300-kDa mannose 6-phosphate receptor cytoplasmic domain by 47-kDa tail-interacting protein. *Proc. Natl. Acad. Sci. USA.* 97:9047–9051.

Peter, B.J., H.M. Kent, I.G. Mills, Y. Vallis, P.J.G. Butler, P.R. Evans, and H.T. McMahon. 2004. BAR domains as sensors of membrane curvature: the amphiphysin BAR structure. *Science.* 303:495–499.

Press, B., Y. Feng, B. Hoflack, and A. Wandinger-Ness. 1998. Mutant rab7 causes the accumulation of cathepsin D and cation independent mannose 6-phosphate receptor in an early endocytic compartment. *J. Cell Biol.* 140: 1075–1089.

Puertollano, R., R.C. Aguilar, I. Gorshkova, R.J. Crouch, and J.S. Bonifacino. 2001. Sorting of mannose 6-phosphate receptors mediated by the GGAs. *Science.* 292:1712–1716.

Puertollano R., N.N. van der Wel, L.E. Greene, E. Eisenberg, P.J. Peters, and J.S. Bonifacino 2003. Morphology and dynamics of clathrin/GGA1-coated carriers budding from the trans-Golgi network. *Mol. Biol. Cell.* 14:1545–1557.

Raiborg, C., K.G. Bache, D.J. Gillooly, I.H. Madshus, E. Stang, and H. Stenmark. 2002. Hrs sorts ubiquitinated proteins into clathrin-coated microdomains of early endosomes. *Nat. Cell Biol.* 4:394–398.

Raiborg, C., T.E. Rusten, and H. Stenmark. 2003. Protein sorting into multivesicular endosomes. *Curr Opin. Cell Biol.* 15:446–455.

Raposo, G., D. Tenza, D.M. Murphy, J.F. Berson, and M.S. Marks. 2001. Distinct protein sorting and localization to premelanosomes, melanosomes, and lysosomes in pigmented melanocytic cells. *J. Cell Biol.* 152:809–824.

Reddy, J.V., and M.N.J. Seaman. 2001. Vps26p, a component of retromer, directs the interactions of Vps35p in endosome-to-Golgi retrieval. *Mol. Biol. Cell.* 12:3242–3256.

Rijnboutt, S., W. Stoorvogel, H.J. Geuze, and G.J. Strous. 1992. Identification of subcellular compartments involved in biosynthetic processing of cathepsin D. *J. Biol. Chem.* 267:15665–15672.

Rohrer, J., A. Schweizer, K.F. Johnson, and S. Kornfeld. 1995. A determinant in the cytoplasmic tail of the cation-dependent mannose 6-phosphate receptor prevents trafficking to lysosomes. *J. Cell Biol.* 130:1297–1306.

Runquist, E.A., and R.J. Havel. 1991. Acid hydrolases in early and late endosome fractions from rat liver. *J. Biol. Chem.* 266:22557–22563.

Sachse, M., S. Urbé, V. Oorschot, G.J. Strous, and J. Klumperman. 2002. Bilayered clathrin coats on endosomal vacuoles are involved in protein sorting toward lysosomes. *Mol. Biol. Cell.* 13:1313–1328.

Sahagian, G.G., J. Distler, and G.W. Jourdian. 1981. Characterization of a membrane-associated receptor from bovine liver that binds phosphomannosyl residues of bovine testicular β-galactosidase. *Proc. Natl. Acad. Sci. USA.* 78: 4289–4293.

Seaman, M.N.J., and H.P. Williams. 2002. Identification of the functional domains of yeast sorting nexins Vps5p and Vps17p. *Mol. Biol. Cell.* 13:2826–2840.

Seaman, M.N.J., E.G. Marcusson, J.L. Cereghino, and S.D. Emr. 1997. Endosome to Golgi retrieval of the vacuolar protein sorting receptor, Vps10p, requires the function of VPS29, VPS30 and VPS35 gene products. *J. Cell Biol.* 137:79–92.

Seaman, M.N.J., J.M. McCaffery, and S.D. Emr. 1998. A membrane coat complex essential for endosome-to-Golgi retrograde transport in yeast. *J. Cell Biol.* 142:665–681.

Seeger, M., and G.S. Payne. 1992. A role for clathrin in the sorting of vacuolar proteins in the Golgi complex of yeast. *EMBO J.* 11:2811–2818.

Stenmark, H., R.G. Parton, O. Steele-Mortimer, A. Lutcke, J. Gruenberg, and M. Zerial. 1994. Inhibition of rab5 GTPase activity stimulates membrane fusion in endocytosis. *EMBO J.* 13:1287–1296.

Takatsu, H., Y. Katoh, Y. Shiba, and K. Nakayama. 2001. Golgi-localizing, γ-adaptin ear homology domain, ADP-ribosylation factor-binding (GGA) proteins interact with acidic dileucine sequences within the cytoplasmic domains of sorting receptors through their Vps27p/Hrs/STAM (VHS) domains. *J. Biol. Chem.* 276:28541–28545.

Varlamov, O., and L.D. Fricker. 1998. Intracellular trafficking of metallocarboxypeptidase D in AtT-20 cells: localization to the trans-Golgi network and recycling from the cell surface. *J. Cell Sci.* 111:877–885.

Waguri, S., F. Dewitte, R. Le Borgne, Y. Rouille, Y. Uchiyama, J.F. Dubremetz, and B. Hoflack. 2003. Visualization of TGN to endosome trafficking through fluorescently labeled MPR and AP-1 in living cells. *Mol. Biol. Cell.* 14:142–155.

Wan, L., S.S. Molloy, L. Thomas, G. Li, Y. Xiang, S.L. Rybak, and G. Thomas. 1998. PACS-1 defines a novel gene family of cytosolic sorting proteins required for trans-Golgi network localization. *Cell.* 94:205–216.

Wang, Y., Y. Zhou, K. Szabo, C.R. Haft, and J. Trejo. 2002. Down-regulation of protease-activated receptor is regulated by sorting nexin 1. *Mol. Biol. Cell.* 13:1965–1976.

Yeung, B.G., H.L. Phan, and G.S. Payne. 1999. Adaptor complex-independent clathrin function in yeast. *Mol. Biol. Cell.* 10:3643–3659.

Zhdankina, O., N.L. Strand, J.M. Redmond, and A.L. Boman. 2001. Yeast GGA proteins interact with GTP-bound Arf and facilitate transport through the Golgi. *Yeast.* 18:1–18.

Zhong, Q., C.S. Lazar, H. Tronchere, T. Sato, T. Meerloo, M. Yeo, Z. Songyang, S.D. Emr, and G. Gill. 2002. Endosomal localization and function of sorting nexin 1. *Proc. Natl. Acad. Sci. USA.* 99:6767–6772.

Zhu, Y., B. Doray, A. Poussu, V.P. Lehto, and S. Kornfeld. 2001. Binding of GGA2 to the lysosomal enzyme sorting motif of the mannose 6-phosphate receptor. *Science.* 292:1716–1718.